Journal of Biological Dynamics
Vol. 3, No. 6, November 2009, 551–573

Taylor & Francis
Taylor & Francis Group

Pattern formation in prey-taxis systems

J.M. Lee[a]*, T. Hillen[a] and M.A. Lewis[a,b]

[a]*Centre for Mathematical Biology, Department of Mathematical and Statistical Sciences, University of Alberta, Edmonton, Alberta, Canada T6G 2G1;* [b]*Centre for Mathematical Biology, Department of Biological Sciences, University of Alberta, Edmonton, Alberta, Canada T6G 2E9*

(*Received 3 July 2007; final version received 27 December 2008*)

In this paper, we consider spatial predator–prey models with diffusion and prey-taxis. We investigate necessary conditions for pattern formation using a variety of non-linear functional responses, linear and non-linear predator death terms, linear and non-linear prey-taxis sensitivities, and logistic growth or growth with an Allee effect for the prey. We identify combinations of the above non-linearities that lead to spatial pattern formation and we give numerical examples. It turns out that prey-taxis stabilizes the system and for large prey-taxis sensitivity we do not observe pattern formation. We also study and find necessary conditions for global stability for a type I functional response, logistic growth for the prey, non-linear predator death terms, and non-linear prey-taxis sensitivity.

Keywords: predator–prey models; prey-taxis; stability; pattern formation; biological control

AMS Subject Classification: 92C15; 92D25; 92D40; 34D23

1. Introduction

There are basically three mechanisms for spatial pattern formation in systems of two reaction–advection–diffusion equations; the Turing patterns [25], chemotaxis patterns [12], and patterns created through reaction kinetics, e.g. the Brusselator [15]. Turing patterns typically arise for a fast inhibitor and a slow activator. Chemotaxis patterns are based upon aggregation towards a chemical signal.

For a predator–prey system without prey-taxis, Okubo and Levin [26] note that an Allee effect in the functional response and a density-dependent death rate of the predator are necessary to generate spatial patterns. The inclusion of species migration (constant flow) as an additional transport process may also increase the possibility of pattern formation [13]. The directional movement of zooplankton plays a role in generating patterns in a plankton community model [22]. For the same system, diffusion also generates pattern formation, and the combined effects of diffusion and velocity result in spatial pattern and an instability like travelling waves, i.e. travelling patchy distributions [23]. Indeed, the magnitude of the relative flow velocity determines the flow-induced

*Corresponding author. Email: jungmin@bio-math10.biology.kyushu-u.ac.jp

ISSN 1751-3758 print/ISSN 1751-3766 online

DOI: 10.1080/17513750802716112
http://www.informaworld.com

instability [28]. Various travelling wave solutions have been studied with similar systems [4,18,33]. In particular, [4,33] also considered escaping behaviours of prey from predation.

For chemotaxis models, spatial patterns have been studied analytically and numerically (see, for example, [7,35,36]). In contrast to the rich development of chemotaxis models, the pattern formation of prey-taxis models is still open to wide investigations. Lewis [20] studied pattern formation in plant and herbivore dynamics and herbivory-taxis was seen to reduce the likelihood of pattern formation. Arditi *et al.* [3] and Chakraborty *et al.* [6] considered a different aspect of predator response to the prey distribution that the velocity of the predators is dependent on prey density.

The goal of this paper is to investigate the contribution of predator and prey movements to spatial pattern formation in predator–prey systems. In particular, we consider foraging behaviour of predators that move towards high prey density. For that, we extend the predator–prey diffusion–reaction model in [27] by incorporating the concept of prey-taxis [14].

1.1. *The model*

A prey-taxis model was derived by Kareiva and Odell in [14], and they studied predator aggregation in high prey density areas. Later the model was applied to estimate the mean travel time of a predator to reach a prey resource [9]. Here we extend the Kareiva and Odell model to studying pattern formation.

The prey-taxis model discussed below contains both diffusion terms that might lead to Turing-type instabilities and a prey-taxis term that might lead to aggregation of predators on local concentrations of prey. In this paper, we will investigate the relative importance of these effects for spatial pattern formation. Prey-taxis allows predators to search more actively for prey, and can generate different spatial patterns from those formed in models without prey-taxis. Generally speaking, we find that prey-taxis tends to stabilize the predator–prey interactions.

The characteristic feature of prey-taxis equations is that taxis is incorporated as an advection term [14,17]. In this paper, we consider the following prey-taxis model

$$v_t = \epsilon v_{xx} + vf(v) - nh(v,n), \tag{1}$$

$$n_t = n_{xx} - (\chi(v)v_x n)_x + \gamma n(h(v,n) - \delta(n)), \tag{2}$$

where ϵ and γ are positive dimensionless parameters. Here $v(x,t)$ and $n(x,t)$ are prey density and predator density, respectively. $f(v)$ is the per capita prey population growth rate, $h(v,n)$ is the functional response, and $\gamma\delta(n)$ is the mortality rate of the predator without the prey. The prey sensitivity, $\chi(v)$, is a non-negative non-increasing function of the prey density, and as example, we choose $\chi(v) = \chi$, or $\chi(v) = \chi/v$.

To investigate the pattern formation properties of Equations (1) and (2), we first consider (1) and (2) without taxis, i.e. $\chi = 0$. Secondly, we study the full model (1) and (2) with $\chi \neq 0$. In Section 2.1, we study pattern formation for Equations (1) and (2). It turns out that pattern formation crucially depends on the functional forms of functional response $h(v,n)$, on the death rate $\delta(n)$, and on the prey growth kinetics $f(v)$. We investigate typical cases, that are discussed in the literature, see, e.g. [34]. For $h(v,n)$ we consider type I (linear) functional response $h(v,n) = v$, type II (hyperbolic) functional response $h(v,n) = (\alpha+1)/(\alpha+v)v$, linear-ratio functional response $h(v,n) = \nu_0(v/n)$, and hyperbolic-ratio functional response $h(v,n) = \mu v/(dn+v)$. The death rate $\delta(n)$ is either constant $\delta(n) = \delta$ or density-dependent $\delta(n) = \delta + \nu n$. For the prey kinetics, we assume either logistic growth $f(v) = 1 - v$ or an Allee effect $f(v) = K(1-v)(v-a)$. The above parameters α, ν_0, μ, d, ν, K, and a are all positive constants. We summarize the choices of these functions, the corresponding pattern formation results, and the corresponding section in Table 1.

Table 1. The possibility of spatial pattern formation is considered in the spatial predator–prey system (1) and (2) with various functional responses, h, prey population dynamics, f, and predator death rates, δ.

Functional response $h(v,n)$	Death rate $\delta(n)=\delta+\nu n$	Prey growth $f(v)$	Pattern formation without taxis	Pattern formation with diffusion and taxis	Section
Linear	Density-dependent ($\nu\neq 0$)	Allee	Yes	Yes for small taxis	2.1 and 2.2
Linear ratio	Constant ($\nu=0$)	Logistic	No	No	2.3
Hyperbolic ratio	Constant ($\nu=0$)	Logistic	Yes	Yes for small taxis	2.4
Hyperbolic	Density-dependent ($\nu\neq 0$)	Logistic	Yes	Yes for small taxis	2.5
Hyperbolic	Constant ($\nu=0$)	Logistic	No	No	2.6
Linear	Density-dependent ($\nu\neq 0$)	Logistic	No	No	2.7

Note: We study type I (linear) functional response of the form $h(v,n)=v$, type II (hyperbolic) functional response of the form $h(v,n)=(\alpha+1)/(\alpha+v)v$, linear ratio functional response of the form $h(v,n)=v_0(v/n)$, and hyperbolic-ratio functional response of the form $h(v,n)=\mu v/(dn+v)$. Constant death rate means $\delta(n)=\delta$ and density-dependent death rate means $\delta(n)=\delta+\nu n$. For logistic growth rate, we have $f(v)=1-v$ and for an Allee effect we have $f(v)=K(1-v)(v-a)$. The parameters α, v_0, μ, d, ν, K, and a are all positive constants.

In Section 3 we consider global stability of the system (1) and (2) with a type I functional response, density-dependent predator death rate, logistic prey growth rate, and a prey-taxis term. We construct a Lyapunov functional and find that for some condition the coexistence steady state is globally stable. We finish the paper with a discussion and suggestions for further studies (Section 4).

Note that in this paper we implement efficient and accurate numerical methods for each term via a fractional step method [19,36] by using MATLAB. For diffusion and reactions terms, we use the Crank–Nicolson scheme and a second-order Runge–Kutta scheme, respectively [1,32]. For the advection term, we use a high-resolution central scheme [16].

2. Pattern formation in prey-taxis systems

In this section we focus on constant prey-taxis $\chi(v)=\chi$ and study Equations (1) and (2) on an interval $[0,L]$ with homogeneous Neumann boundary conditions given by

$$v_x(0,t)=0,\quad v_x(L,t)=0,\quad n_x(0,t)=0,\quad n_x(L,t)=0. \tag{3}$$

We first consider Equations (1) and (2) for general $f(v)$, $h(v,n)$, and $\delta(n)$ and study the specific functional forms later. Since we are interested in understanding biological phenomena, the prey growth function $f(v)$ can be negative with an Allee effect, but the functional response $h(v,n)$ is assumed non-negative. We assume that a non-trivial coexistence steady state (v_s,n_s) exists.

In order to investigate pattern formation, we follow the standard Turing stability analysis (see [25,17] for details).

We first assume that (v_s,n_s) is linearly stable for the purely kinetic equations.

ASSUMPTION

$$A+D<0,\quad AD-BC>0, \tag{4}$$

where

$$\begin{aligned} A&=(v_s f'(v_s)+f(v_s)-n_s h_v(v_s,n_s)),\\ B&=-h(v_s,n_s)-n_s h_n(v_s,n_s),\\ C&=\gamma n_s h_v(v_s,n_s),\\ D&=\gamma(h(v_s,n_s)+n_s h_n(v_s,n_s)-\delta(n_s)-n_s\delta'(n_s)). \end{aligned} \tag{5}$$

Assumption (4) *guarantees linear stability of* (v_s, n_s).

Now, we consider the full reaction–taxis–diffusion system (1) and (2) and obtain the following characteristic equation for an eigenvalue λ of the linearization at (v_s, n_s):

$$\lambda^2 - M_1(k^2)\lambda + M_2(k^2) = 0, \tag{6}$$

where

$$M_1(k^2) = A + D - (1+\epsilon)k^2, \tag{7}$$

and

$$M_2(k^2) = AD - BC + \epsilon k^4 - (A + \epsilon D + B\chi n_s)k^2, \tag{8}$$

where A, B, C, and D are defined in equation (5) and k denotes the wave number. Non-negative ϵ and k^2 guarantee $M_1(k^2) \leq A + D < 0$ for all k, so the only way $\lambda(k^2)$ can be positive is the case that $M_2(k^2) < 0$ for some k^2. Hence, a necessary condition for pattern formation is $A + \epsilon D + B\chi n_s > 0$. Due to negative B (see Equation (5)), indeed positive χ tends to inhibit $A + \epsilon D + B\chi n_s$ from becoming positive, as shown in the following lemma.

LEMMA 2.1 *Assume that* A, B, C, *and* D *are defined in Equation* (5) *and* ϵ *is positive. In addition, if* $AD - BC > 0$ *is assumed as in Equation* (4), *then there exists* $\chi^* \geq 0$ *such that* $M_2(k^2) > 0$ *for all* k *and all* $\chi \geq \chi^*$. *In this case, the homogeneous solution* (v_s, n_s) *is linearly stable.*

Proof Since $AD - BC > 0$ and $\epsilon > 0$, positive $-(A + \epsilon D + B\chi n_s)$ guarantees that $M_2(k^2) > 0$. From the expression $A + \epsilon D + B\chi n_s = 0$, we can isolate χ and set this χ as χ_0. Then we have $\chi_0 = -(A + \epsilon D)/Bn_s > 0$. We now define $\chi^* = \max(\chi_0, 0)$. We have $\chi^* \geq 0$ and for all $\chi \geq \chi^*$, we have $M_2(k^2) > 0$ independent of the value k. ■

Therefore, prey-taxis tends to reduce the occurrence of dispersal-induced instability. It is indeed the predator diffusion that is crucial to dispersal-induced instability. When prey act anti-predator defensive behaviours such as kicking and attacking and show chemical defences [21], predators may retreat from high prey area, in which case χ in Equation (8) can be negative. As a result, a predator–prey system may generate pattern formation. But here we do not consider this case in detail. In the absence of predators, the prey diffusion would reduce local prey maxima and equilibrate the prey distribution. If predators are present and if they are attracted to local prey maxima through prey-taxis, then the reduction of local prey maxima is enhanced. Hence, if the taxis component is strong enough, we might not expect pattern formation. This is indeed the case, as given in Lemma 2.1. For a specific example, we refer to Section 2.2.

In the following subsections, we consider specific choices for the functional responses, h, the death rate of the predator, δ, and prey growth rate, f. The ability of the prey taxis model (1) and (2) to exhibit a spatial pattern crucially depends on the parameter functions $h(v, n)$, $\delta(n)$, and $f(v)$. Thus, in this section, we study various typical cases separately. An overview of the cases and the corresponding results is given in Table 1.

2.1. *Type I functional response, density-dependent predator death rate, and Allee effect with diffusion only*

In this subsection, we show that pattern formation is possible when there is a type I functional response and an Allee effect along with a density-dependent predator death rate (Table 1, row 1).

We consider an Allee effect on the prey population dynamics $f(v) = K(1-v)(v-a)$ with $0 < a < 1$ and $K = 4/(1-a)^2$, a type I functional response, $h(v,n) = v$, a density-dependent predator death rate, $\delta(n) = \delta + \nu n$, $\nu \geq 0$, and no taxis, i.e. $\chi = 0$. Here the parameter a is a threshold, below which the prey population declines. Okubo and Levin [26] argued that a predator–prey model with dispersal may generate diffusion-driven instability if the mortality of the predator depends on the population density and the per-capita growth rate of the prey is determined by an Allee effect. Note that the trivial steady state $(v,n) = (0,0)$ is locally stable because for $(v,n) = (0,0)$ the characteristic polynomial for purely kinetic equations has two negative eigenvalues, $\lambda = -\gamma\delta$ and $\lambda = -Ka$. We assume biologically relevant parameters in the region $0 < \delta < 1$ and $0 < a < 1$. For the prey-only steady state $(v,n) = (1,0)$, the characteristic polynomial has one positive eigenvalue $\lambda = \gamma(1-\delta)$ and one negative eigenvalue $\lambda = -K(1-a)$.

For the homogeneous coexistence steady state (v_s, n_s), we find

$$A = Kv_s(1+a-2v_s), \quad B = -v_s, \quad C = \gamma n_s, \quad D = -\gamma n_s \nu, \tag{9}$$

and $M_1(k^2)$ and $M_2(k^2)$ are given by

$$M_1(k^2) = A + D - (1+\epsilon)k^2, \tag{10}$$

$$M_2(k^2) = AD - BC + \epsilon k^4 - (A + \epsilon D)k^2. \tag{11}$$

It is noted that the sign of A depends on the sign of $1 + a - 2v_s$.

Here we set $\bar{v} = (1+a)/2$. Hence, when $v_s > \bar{v}$, A is negative and when $v_s < \bar{v}$, A is positive. Recall that the coexistence steady state (v_s, n_s) comes from the intersection of the two nullclines: $v - \delta - \nu n = 0$ and $K(1-v)(v-a) - n = 0$ (see Figure 1).

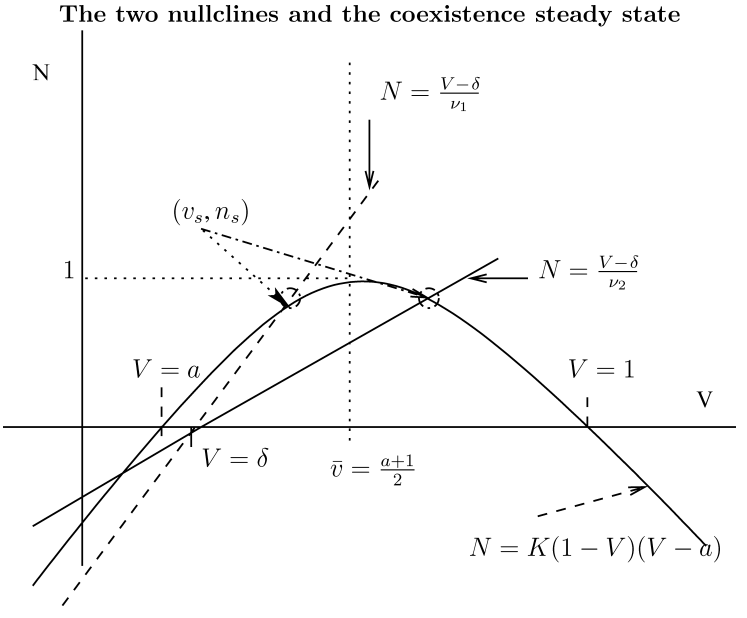

Figure 1. The v-nullcline $N = K(1-V)(V-a)$ is shown as a solid curve. For two values of ν, we show the corresponding n-nullcline, $N = (V-\delta)/\nu$ as a dashed line and a solid line. The equilibrium (v_s, n_s) is the intersection of the nullclines. We have chosen two values of ν so that $v_s < \bar{v}$ for ν_1 and $v_s > \bar{v}$ for ν_2 with $\nu_1 < \nu_2$.

First, we consider $v_s > (1+a)/2$. Since $v_s > \bar{v}$, we find that at $v = v_s$ the v-nullcline is above the n-nullcline. This means that $K(1-\bar{v})(\bar{v}-a) > (\bar{v}-\delta)/\nu$, which translates into the condition

$$a + 1 < 2(\delta + \nu).$$

For this case we prove stability.

LEMMA 2.2 *Assume that* $h(v,n) = v$, $\delta(n) = \delta + \nu n$, $f(v) = K(1-v)(v-a)$, *and* $\chi = 0$. *If* $a + 1 < 2(\delta + \nu)$, *then no pattern formation occurs about the coexistence steady state* (v_s, n_s) *for the system* (1) *and* (2).

Proof The condition $a + 1 < 2(\delta + \nu)$ implies that $v_s > (1+a)/2$. Hence $A < 0$. In addition, we find $B < 0$, $C > 0$, and $D < 0$ and $A < 0$, $B < 0$, and $D < 0$ imply $M_2(k^2) = AD - BC + \epsilon k^4 - (A\epsilon + D)k^2 > 0$ for all real k. Hence, we cannot expect diffusion-taxis-driven instability about the coexistence steady state. ■

In Figure 1 it is noted that v_s should be between a and 1, i.e. $a < v_s < 1$, otherwise n_s is negative. In Lemma 2.2, we considered that $v_s > (1+a)/2$ and found no pattern. Thus we now consider $a < v_s < \bar{v} = (1+a)/2$. First we investigate how many v_s may exist between a and $\bar{v}$, and then we find conditions for the existence of v_s between a and $\bar{v}$.

The v values for the coexistence steady state are obtained from

$$K\nu v^2 - (K\nu(1+a) - 1)v + K\nu a - \delta = 0. \tag{12}$$

When $a < \delta$, Figure 1 shows that Equation (12) has two real roots. Indeed, for the root less than a, n_s would be negative, which is not biologically relevant. Hence, when $a < \delta$, Equation (12) has one biologically relevant root. In addition, $v_s < \bar{v}$ leads to $a > 2(\delta + \nu) - 1$. Therefore, for

$$2(\delta + \nu) - 1 < a < \delta, \tag{13}$$

the biologically relevant coexistence state exists and its v value is located between $\delta < v_s < \bar{v}$.

When $a > \delta$, we may expect two positive roots from Equation (12). However, a simple computation of Equation (12) shows that we cannot have two positive roots. Under assumption (13), the biologically relevant solution of Equation (12) is given by

$$v_s = \frac{K\nu + K\nu a - 1 + \sqrt{K^2\nu^2a^2 + (-2K\nu - 2K^2\nu^2)a + K^2\nu^2 + 1 - 2K\nu + 4K\nu\delta}}{2K\nu}. \tag{14}$$

The discriminant in Equation (14) is zero for

$$\underline{v} = \frac{K\nu + K\nu a - 1}{2K\nu} = \frac{1+a}{2} - \frac{1}{2K\nu}. \tag{15}$$

Equations (14) and (15) give a condition for the existence of the coexistence steady state,

$$v_s \geq \underline{v} = \frac{1+a}{2} - \frac{(1-a)^2}{8\nu},$$

which will be used to show that $AD - BC > 0$, whenever v_s exists.

We find $A > 0$ from the condition (13). Additionally, from Equation (9) we find $B < 0$, $C > 0$, and $D < 0$. The stability condition $A + D < 0$ leads to a condition

$$Kv_s(1 + a - 2v_s) < \gamma(v_s - \delta). \tag{16}$$

In Figure 2 we plot the left- and right-hand sides of Equation (16) as a function of v_s.

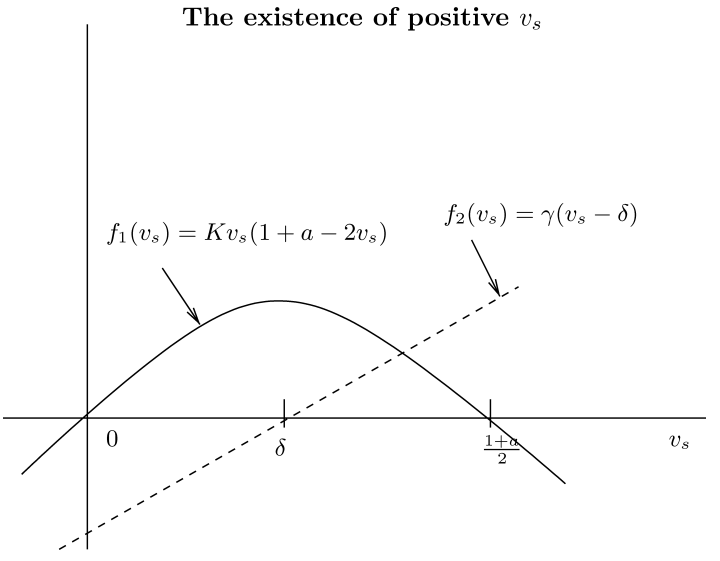

Figure 2. Plot of the left- and right-hand sides of Equation (16) as function of v_s. The region of $A + D < 0$ is where the dashed line lies above the curve.

As γ varies from zero to infinity, the intersection of $Kv_s(1 + a - 2v_s)$ and $\gamma(v_s - \delta)$ changes from $v_s = (1 + a)/2$ to $v_s = \delta$. Given a value for v_s, we can always choose γ small enough such that condition (16) is not true. Thus, γ should be greater than a minimum value, γ_0. Here $\gamma_0 = Kv_s(1 + a - 2v_s)/(v_s - \delta)$, where v_s is computed in Equation (14). Therefore, for $\gamma > \gamma_0$, we have $A + D < 0$.

Thus a biologically relevant v_s is in the interval

$$\max\left(\delta, \frac{1+a}{2} - \frac{(1-a)^2}{8\nu}\right) \leq v_s < \frac{a+1}{2}. \tag{17}$$

We found that Equation (17) holds under assumption (13).

THEOREM 2.3 *Assume that* $h(v, n) = v$, $\delta(n) = \delta + \nu n$, $f(v) = K(1 - v)(v - a)$, *and* $\chi = 0$. *If a satisfies condition* (13), *then* (i) *the coexistence steady state* (v_s, n_s) *exists*, (ii) $AD - BC > 0$, (iii) *if in addition, there exists* $\epsilon_1 > 0$ *such that for each* $\epsilon < \epsilon_1$ *there exists a non-empty interval* $[k_1, k_2]$ *of unstable modes, so we may expect diffusion-driven instability about the coexistence steady state, and* (iv) *if* $\epsilon > \epsilon_1$, *then* (v_s, n_s) *is linearly stable.*

Proof

(i) It was shown that condition (13) implies the existence of a unique positive root v_s.

(ii) When a positive v_s exists, v_s satisfies condition (17). Now we consider the condition for $AD - BC > 0$.

$$\begin{aligned} AD - BC &= -Kv_s(1 + a - 2v_s)\gamma n_s \nu + \gamma n_s v_s \\ &= \gamma n_s v_s(1 - K\nu(1 + a - 2v_s)) > 0, \end{aligned}$$

which holds if $v_s > (1 + a)/2 + 1/2K\nu$. Indeed, this is true by condition (17). Therefore, $AD - BC$ is always positive under the assumption of the existence of a coexistence steady state.

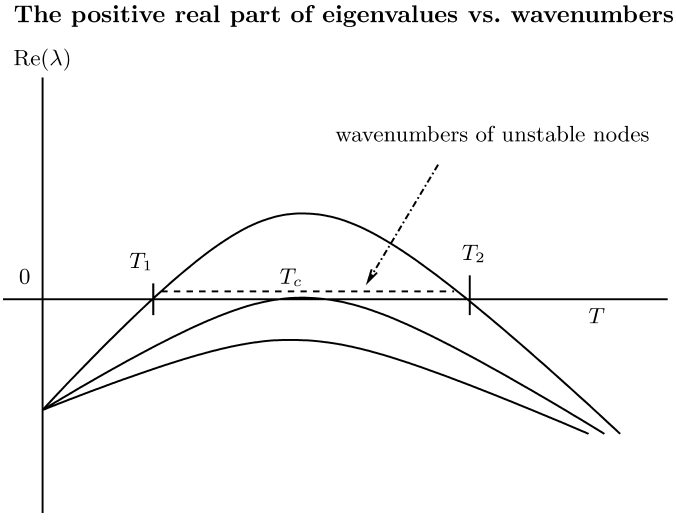

Figure 3. Plot of the eigenvalue $\lambda(k^2)$ as a function of T with $T = k^2$.

(iii) $M_1(k^2)$ and $M_2(k^2)$ are given by Equations (10) and (11), respectively, with $A = Kv_s(1 + a - 2v_s)$, $B = -v_s < 0$, $C = \gamma n_s > 0$, and $D = -\gamma n_s \nu < 0$.

Hence, $A + D < 0$ guarantees $M_1(k^2) = A + D - (1 + \epsilon)k^2 < 0$. If $\epsilon \geq 1$, then $D < 0$ gives $A + D\epsilon \leq A + D < 0$, hence $M_2(k^2)$ is always positive. On the other hand, setting $\epsilon_0 = Kv_s(1 + a - 2v_s)/\gamma(v_s - \delta)$, for $\epsilon < \epsilon_0$, we have $A + D\epsilon > 0$ and $M_2(k^2)$ can be negative for some k.

Setting $T = k^2$, the quadratic equation $M_2(T) = 0$ may have two roots, $T_{1,2}$ (see Figure 3). By solving this quadratic equation, it can be shown that for $\epsilon < \epsilon_1$ there exist real k_1 and k_2. For unstable modes $k \in [k_1, k_2]$ with $k_1 = \sqrt{T_1}$ and $k_2 = \sqrt{T_2}$, we have Re(λ)> 0. Hence we may expect diffusion-driven instability about the coexistence steady state (see also [30]).

(iv) If $\epsilon > \epsilon_1$, then $M_2(k^2)$ is always positive for all k. Hence we cannot expect diffusion-driven instability about the coexistence steady state. ■

Segel and Jackson [30] also considered diffusion-driven instability in a predator–prey interaction. They used $\delta(n) = \nu n$ and $f(v) = 1 + Kv$, and found the wavelength of the instability (see also [26] for general discussion on diffusion-driven instability in a predator–prey interaction).

In particular, for $\epsilon \ll 1$, we apply a perturbation method to approximate two values $T_{1,2}$, that is, $T_1 = (AD - BC)/A$ and $T_2 = A/\epsilon$. Therefore, for $(AD - BC)/A < T < A/\epsilon$, $M_2(T)$ is negative.

For example, we consider an interval $[0, L]$ with homogeneous Neumann boundary condition given by Equation (3). If $k(n) = n\pi/L$ in $[k_1, k_2]$ with positive integer n, then pattern formation occurs. Thus, we can calculate a minimum domain size for pattern formation. Since $k_1 < k(n) < k_2$, we substitute $k(n) = n\pi/L$ and rearrange the inequality with respect to L. Then we have

$$\frac{n\pi}{k_2} < L < \frac{n\pi}{k_1},$$

which should hold for some integer n. Therefore, the minimum length for possible instabilities is $L^* = \pi/k_2$, and for $L < \pi/k_2$, we cannot expect pattern formation.

In Figure 4, we show phase portraits of the predator–prey system (1) and (2) without dispersal terms. As γ increases, the coexistence steady state bifurcates from an unstable spiral to a stable

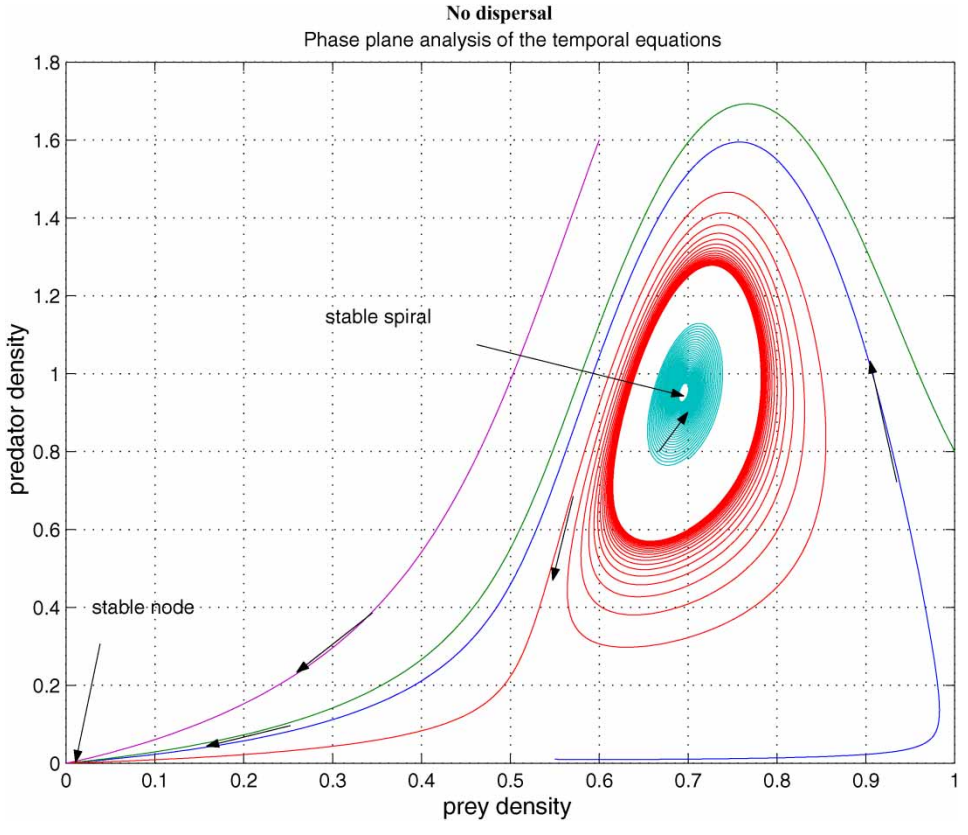

Figure 4. Coexistence steady state is shown to be locally asymptotically stable for system (1) and (2) without dispersal terms and with $f(v) = 16(1-v)(v-0.5)$, $h(v,n) = v$, and $\delta(n) = 0.6 + 0.1n$. Time step is $dt = 0.01$ and $\gamma = 13$. Here the coexistence steady state is $(v_s, n_s) = (0.695, 0.952)$. Available in colour online.

spiral. From simulations with various γ, it is noted that an unstable limit cycle occurs for a certain range of γ. When γ is smaller than the lower bound of this range, the coexistence steady state is an unstable spiral. When γ is bigger than the upper bound of the range, the coexistence steady state is a stable spiral with non-empty basin of attraction. Figure 5 shows that the stable coexistence steady state without dispersal terms becomes unstable if diffusion terms are introduced. As a result, patterns are generated. We demonstrate a snapshot of the asymptotic prey and predator distributions in Figure 6. It is noted that high prey density area seems to attract more predators. Moreover, the patch size of prey is seen to be an important factor to attract more predators.

2.2. *Type I functional response, density-dependent predator death rate, and Allee effect with diffusion and prey-taxis*

We now include prey-taxis in the calculations of the previous subsection (Table 1, row 1). We consider the reaction–diffusion–taxis system (1) and (2) for $\chi(v) = \chi$. We consider Allee-type growth for the prey, $f(v) = K(1-v)(v-a)$ with $0 < a < 1$ and $K = 4/(1-a)^2$, a type I functional response, $h(v,n) = v$, and a density-dependent predator death rate, $\delta(n) = \delta + \nu n$. We have shown in the previous subsection that for $\chi = 0$, pattern formation may occur. In this subsection, we consider how the conditions of pattern formation change if χ is introduced.

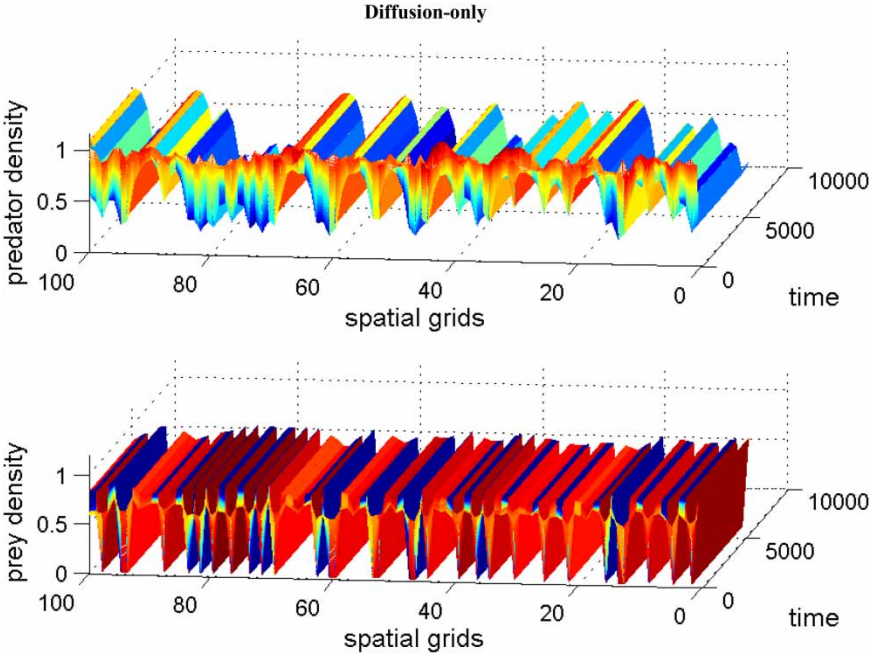

Figure 5. Coexistence steady state is shown to be locally unstable for system (1) and (2) with $\chi(v) = 0.0$, $f(v) = 16(v - 0.5)(1 - v)$, $h(v, n) = v$, and $\delta(n) = 0.6 + 0.1n$. Spatial grid size is $dx = 0.25$, time step $dt = 0.01$, and $\gamma = 14$ with 60 time units. The diffusion coefficient ϵ is 0.01. Here the coexistence steady state is $(v_s, n_s) = (0.695, 0.952)$. Available in colour online.

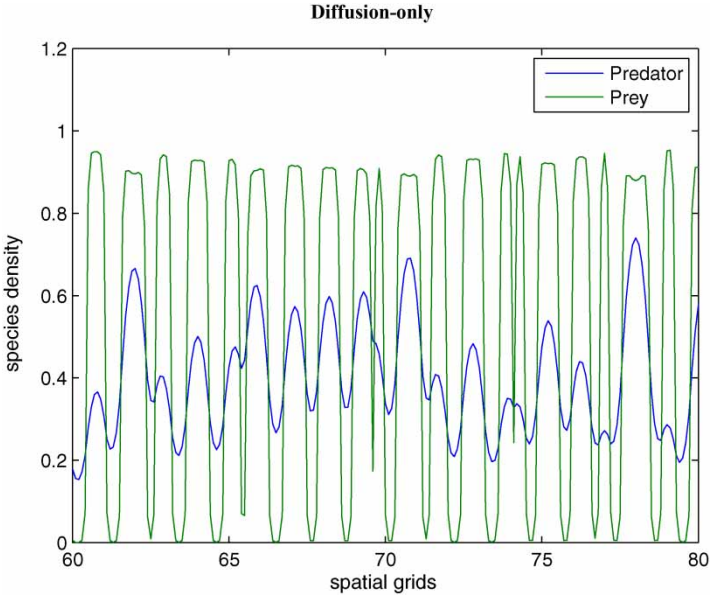

Figure 6. With the same parameters as in Figure 5, we demonstrate a snapshot of the spatial prey and predator distributions after 60 time units between dimensionless spatial locations 10 and 15. Available in colour online.

LEMMA 2.4 *Assume* a, δ, *and* ϵ *satisfy instability conditions of Theorem* 2.3. *Then from Lemma* 2.1 *we compute*

$$\chi^* = \frac{K v_s(1 + a - 2v_s) + \epsilon\gamma(v_s - \delta)}{v_s n_s}$$

such that the coexistence steady state (v_s, n_s) *for system* (1) *and* (2) *is linearly stable for each* $\chi \geq \chi^*$. *For* $\chi < \chi^*$, *there exists an interval* $[k_1, k_2]$ *of unstable modes.*

Proof Here $M_1(k^2)$ from (7) is the same as in the case of diffusion-only (10) so that it is negative for all k. But $M_2(k^2)$ from (8) is different by the term $B\chi n_s$. Setting $M_2(k^2) = 0$ and $T = k^2$, we obtain after rearrangements

$$\epsilon T^2 - (A + \epsilon D)T + AD - BC = B\chi n_s T. \tag{18}$$

Figure 7 shows three typical situations of intersections of the left- hand and the right-hand sides of Equation (18). In the diffusion-only case, we saw that there may be two roots, T_1 and T_2, of $\epsilon T^2 - (A + \epsilon D)T + AD - BC = 0$ under the conditions that $A + \epsilon D > 0$. Between $T_1 < T < T_2$, $\epsilon T^2 - (A + \epsilon D)T + AD - BC$ is negative. In order for $M_2(T)$ to be negative, the left-hand side of Equation (18) should be less than the right-hand side. In Figure 7, the region $T_3 < T < T_4$ where the solid curve is below the dashed line makes $M_2(T)$ negative. As we can see in Figure 7, T_3 is always greater than T_1 and T_4 smaller than T_2 for positive χ.

As χ gets bigger, the slope of the line of the right-hand side of Equation (18) is steeper so that for $\chi \geq \chi^*$ there will be no intersection of the curve and the line (see Figure 7). In that case, $M_2(T)$ is always non-negative, which leads to negative eigenvalues and to stability. In Theorem 2.3, for $\chi = 0$, we found a threshold of $\epsilon_0 = K v_s(1 + a - 2v_s)/\gamma(v_s - \delta)$. For $\chi \neq 0$, the threshold for pattern formation is

$$\epsilon_1 = \frac{K v_s(1 + a - 2v_s) - v_s \chi n_s}{\gamma(v_s - \delta)} \leq \epsilon_0.$$

Thus, as χ gets bigger, ϵ_1 requires smaller value ϵ for pattern formation. ■

Figure 4 shows that the coexistence steady state for the spatially homogeneous predator–prey system (1) and (2) without dispersal terms is stable. In Figure 5, introducing the diffusion term generates patterns. The numerical simulations confirmed that when we introduce a large prey-taxis term, patterns disappear (not shown here).

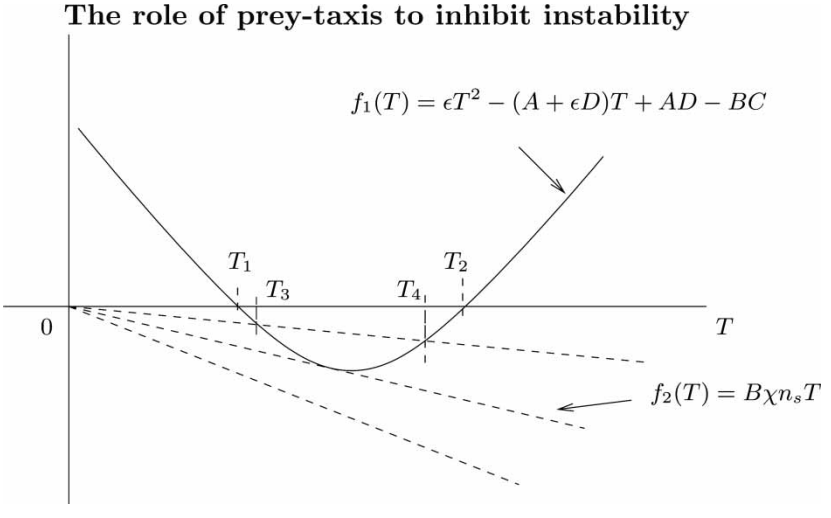

Figure 7. Plot of the left- and right-hand sides of Equation (18) as a function of T with $T = k^2$. The solid curve is from the left-hand side of Equation (18) and the dashed lines are from the right-hand side of Equation (18). As χ increases, the number of intersection changes from zero to two. Note that B is negative.

2.3. *Linear ratio-dependent functional response, constant predator death rate, and logistic growth*

In this subsection, we show that pattern formation is impossible when there is a linear ratio functional response and logistic growth along with a constant predator death rate (Table 1, row 2). We consider the linear ratio-dependent functional response, $h(v, n) = \nu_0(v/n)$, with logistic growth for the prey, $f(v) = 1 - v$, and a constant predator death rate, $\delta(n) = \delta$, and ν_0 is a constant parameter. Thus the coexistence steady state is now $(v_s, n_s) = (1 - \nu_0, \nu_0/\delta(1 - \nu_0))$, which is biologically relevant for $0 \leq \nu_0 < 1$. In this case, we obtain

$$A = -(1 - \nu_0), \quad B = 0, \quad C = \gamma\nu_0, \quad D = -\gamma\delta.$$

We observe that $A < 0$, $D < 0$, $B = 0$, $AD - BC > 0$, and $M_2(k^2) = AD - BC + \epsilon k^4 - (A + \epsilon D + B\chi n_s)k^2 > 0$ for all k. Hence, the homogeneous steady state is linearly stable.

LEMMA 2.5 *Assume* $f(v) = 1 - v$, $h(v, n) = \nu_0(v/n)$, *and* $\delta(n) = \delta + \nu n$, *then no pattern formation occurs about the coexistence steady state*, $(v_s, n_s) = (1 - \nu_0, \nu_0/\delta(1 - \nu_0))$, *for system* (1) *and* (2).

2.4. *Hyperbolic ratio-dependent functional response, constant predator death rate, and logistic growth*

We now modify the analysis of the previous subsection to include a hyperbolic ratio rather than linear ratio functional response. This allows for the possibility of pattern formation, providing that taxis is sufficiently small (Table 1, row 3). We consider hyperbolic ratio-dependent functional response, $h(v, n) = \mu v/(dn + v)$ with logistic growth for the prey, $f(v) = 1 - v$, and a constant predator death rate, $\delta(n) = \delta$, and $\mu \geq 0$ and $d \geq 0$ are constants. Thus the coexistence steady state in this case is

$$(v_s, n_s) = \left(\frac{(d - \mu + \delta)}{d}, \frac{(d - \mu + \delta)(\mu - \delta)}{d^2\delta}\right),$$

which is biologically relevant for $\delta < \mu < d + \delta$. In this case, we have

$$A = -\frac{(d\mu - \mu^2 + \delta^2)}{d\mu}, \quad B = -\frac{\delta^2}{\mu}, \quad C = \frac{(\mu - \delta)^2}{d\mu}\gamma, \quad D = -\frac{\delta(\mu - \delta)}{\mu}\gamma.$$

We consider conditions that $A + D < 0$ and $AD - BC > 0$. For $A < 0$, it is seen that $A + D < 0$ and $AD - BC > 0$. For $A > 0$, $\gamma > \gamma_0$, with

$$\gamma_0 = -\frac{(d\mu - \mu^2 + \delta^2)}{d(\mu - \delta)\delta} > 0,$$

implies that $A + D < 0$.

LEMMA 2.6 *Assume* $f(v) = 1 - v$, $h(v, n) = \mu v/(dn + v)$, $\delta(n) = \delta$, *and* $\chi = 0$.

(i) *If* $(d\mu - \mu^2 + \delta^2) > 0$, *no pattern formation occurs about the coexistence steady state*, (v_s, n_s), *for system* (1) *and* (2).
(ii) *Assume* $(d\mu - \mu^2 + \delta^2) < 0$. *There exists* $\epsilon_1 > 0$ *such that for each* $\epsilon < \epsilon_1$ *there exists a non-empty interval* $[k_1, k_2]$ *of unstable modes, so we may expect diffusion-driven instability about the coexistence steady state*,
(iii) *in case* (ii) *if* $\epsilon > \epsilon_1$, *then* (v_s, n_s) *is linearly stable.*

Proof

(i) First, $(d\mu - \mu^2 + \delta^2) > 0$ implies $A < 0$. In addition, $B < 0$, $C > 0$, and $D < 0$ result in positive $M_2(k^2)$ from (11). Hence, we cannot expect diffusion-taxis-driven instability about the coexistence steady state.

(ii) Second, we consider $(d\mu - \mu^2 + \delta^2) < 0$, which gives $A > 0$. It is also seen that $AD - BC > 0$ and for $\gamma > \gamma_0$, $A + D < 0$, which implies that $M_1(k^2)$ from (10) is negative. However, when ϵ is less than $\epsilon_0 = -(d\mu - \mu^2 + \delta^2)/d\gamma(\mu - \delta)\delta$, then $A + \epsilon D$ is positive. Thus, $M_2(k^2)$ can be negative. With the same steps in Theorem 2.3, we can find k_1 and k_2 with $k_{1,2}^2 = (\mu^2 - d\mu - \delta^2 - \epsilon d\mu\gamma\delta + \epsilon d\gamma\delta^2 \mp \sqrt{G_0 + G_1\epsilon + G_2\epsilon^2})/(2\epsilon d\mu)$, where

$$G_0 = (-d\mu + \mu^2 - \delta^2)^2,$$
$$G_1 = 2d(\mu - \delta)\gamma\delta(\mu^2 - d\mu - 2\mu\delta + \delta^2),$$
$$G_2 = \gamma^2\delta^2 d^2(\mu - \delta)^2.$$

Consequently for $\epsilon < \epsilon_1 = (-G_1 - \sqrt{G_1^2 - 4G_0G_2})/2G_2$, there exist real k_1 and k_2. Furthermore, for $k_1 < k < k_2$, we have $\mathrm{Re}(\lambda) > 0$, and we may expect diffusion-driven instability about the coexistence steady state.

(iii) If $\epsilon > \epsilon_1$, then $M_2(k^2)$ is positive for all k. Hence, we cannot expect diffusion-driven instability about the coexistence steady state. ■

Alonso *et al.* [2] also considered a hyperbolic ratio-dependent functional response for pattern formation by using numerical exploration of the parameter space.

Now we can follow the argument of the case including an Allee effect. Thus, the reaction–diffusion system may show diffusion-driven instability depending on parameters μ, d, δ, γ, and ϵ. Furthermore, the prey-taxis term tends to inhibit the occurrence of dispersal-driven instability (see Lemma 2.1 and Section 2.2 for the full argument).

In Figure 8, we show phase portraits of the predator–prey system (1) and (2) with hyperbolic-ratio functional response and without dispersal terms. As γ increases, the coexistence steady state bifurcates from an unstable spiral to a stable spiral. Figure 9 demonstrates that this homogeneous coexistence steady state becomes unstable if diffusion terms are introduced. As a result, patterns are generated. It is shown that when we introduce a large prey-taxis term, patterns eventually disappear (see [17] for figure).

2.5. *Type II functional response, density-dependent predator death rate, and logistic growth*

Next we consider a hyperbolic functional response and a density-dependent predator death rate from the setting of the previous subsection and show that pattern formation is possible, provided that taxis is sufficiently small (Table 1, row 4). We consider type II functional response, $h(v, n) = (\alpha + 1)/(\alpha + v)v$ as in [27], a density-dependent predator death rate, $\delta(n) = \delta + \nu n$, and logistic growth for the prey, $f(v) = 1 - v$ with $\alpha > 0, 0 < \delta < 1$, and $\nu > 0$. The coexistence steady state can be obtained from the root of the following system

$$n = g_1(v) = (1 - v)\frac{(\alpha + v)}{\alpha + 1},$$
$$n = g_2(v) = \frac{((\alpha + 1)/(\alpha + v)v - \delta)}{\nu}.$$

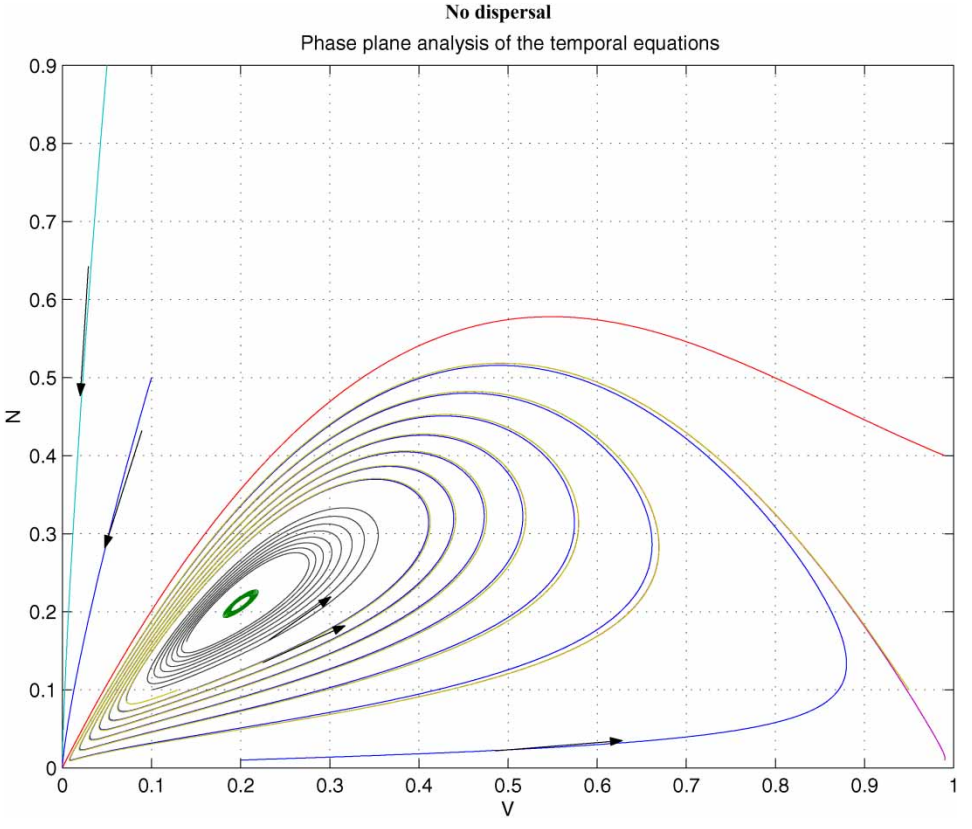

Figure 8. Coexistence steady state is shown to be locally asymptotically stable for system (1) and (2) without dispersal terms and with $h(v, n) = 0.8v/(0.05n + v)$, $f(v) = 1 - v$, and $\delta(n) = 0.76$. Time step is $dt = 0.005$, and $\gamma = 15$. Here the coexistence steady state is $(v_s, n_s) = (0.2, 0.211)$. Available in colour online.

By applying the intermediate-value theorem, it is shown that there is at least one point $v = v_s$ in the open interval $(0, 1)$ such that $g(v_s) = 0$. Moreover, since $n_s = g_1(v_s) > 0$ for $v_s \in (0, 1)$, n_s corresponding to v_s is positive as well.

LEMMA 2.7 *Assume* $f(v) = 1 - v$, $h(v, n) = v(\alpha + 1)/(\alpha + v)$, *and* $\delta(n) = \delta + \nu n$, *then there exists at least one coexistence steady state*, (v_s, n_s), *for the system* (1) *and* (2).

For an homogeneous coexistence steady state (v_s, n_s), we find

$$A = 1 - 2v_s - n_s \frac{(\alpha + 1)\alpha}{(\alpha + v_s)^2}, \quad B = -v_s \frac{\alpha + 1}{\alpha + v_s},$$

$$C = \gamma n_s \frac{(\alpha + 1)\alpha}{(\alpha + v_s)^2}, \quad D = -\gamma n_s \nu.$$

It is noted that $B < 0$, $C > 0$, and $D < 0$. Thus for $A < 0$, we cannot expect spatial pattern because $M_1(k^2) < 0$ and $M_2(k^2) > 0$ for all k. The condition for $A < 0$ is rewritten in terms of parameters α, δ, and ν as follows:

$$\nu > \frac{4(1 - \alpha - \delta)}{\alpha + 1}.$$

Therefore, we can summarize the result.

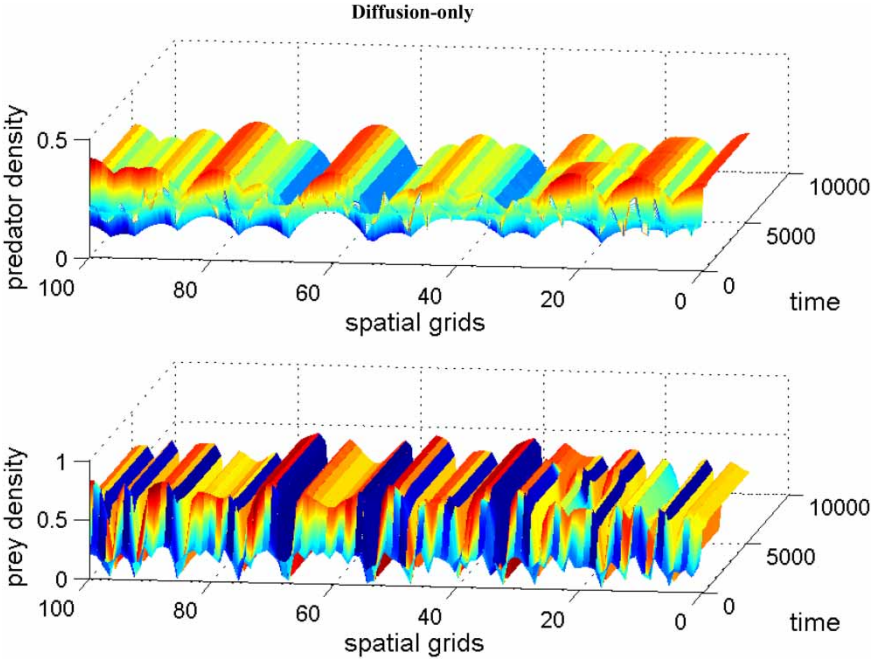

Figure 9. Coexistence steady state is shown to be locally unstable for system (1) and (2) with $h(v,n) = 0.8v/(0.05n + v)$, $f(v) = 1 - v$, and $\delta(n) = 0.76$ and with $\chi(v) = 0.0$. The diffusion coefficient ϵ is 0.01. Spatial grid size is $dx = 0.25$, time step $dt = 0.01$, and $\gamma = 15$. Here the coexistence steady state is $(v_s, n_s) = (0.2, 0.211)$. Available in colour online.

LEMMA 2.8 *Assume* $f(v) = 1 - v$, $h(v,n) = v(\alpha + 1)/(\alpha + v)$, *and* $\delta(n) = \delta + \nu n$. *If* $\nu > 4(1 - \alpha - \delta)/(\alpha + 1)$, *then no pattern formation occurs about the coexistence steady state*, (v_s, n_s), *for the system* (1) *and* (2).

This result was also confirmed numerically for selected parameter values (not shown here). Now we consider the case of $A > 0$, that is,

$$0 < v_s < \frac{1-\alpha}{2}, \text{ equivalently } 0 < \nu < \frac{4(1-\alpha-\delta)}{\alpha+1}.$$

The condition for

$$A + D = \frac{-2v_s^2 + (1 - \alpha - \gamma(1 + \alpha - \delta))v_s + \gamma\delta\alpha}{\alpha + v_s} < 0$$

implies (after some computation)

$$1 - \alpha - \delta > 0. \tag{19}$$

Under condition (19), we set the positive root of $A + D$ expressed above with v^*, and then v^* is between 0 and $(1 - \alpha)/2$. Thus, for v_s in $(v^*, (1 - \alpha)/2)$, we have $A + D < 0$. Note: $v^* = (1 - \alpha - \gamma(1 + \alpha - \delta))/4 + (\sqrt{(1 - \alpha - \gamma(1 + \alpha - \delta))^2 + 8\gamma\delta\alpha})/4$. Recall that v_s is independent of γ, so by controlling γ we can make v^* smaller than v_s.

Now we consider $AD - BC > 0$. Because A is positive, we cannot guarantee $AD - BC > 0$. After rearrangement, we find

$$AD - BC = \gamma n_s \left(-\nu(1 - 2v_s) + (\alpha + 1)\alpha \frac{(2\alpha + 2 - \delta)v_s - \delta\alpha}{(\alpha + v_s)^3} \right),$$

which is positive if

$$G(v_s) = \left(-\nu(1 - 2v_s) + (\alpha + 1)\alpha \frac{(2\alpha + 2 - \delta)v_s - \delta\alpha}{(\alpha + v_s)^3} \right) > 0.$$

After some computation, we obtain that

$$G(0) = -(\alpha + 1)\frac{\delta}{\alpha} - \nu < 0, \quad \text{and} \quad G\left(\frac{1-\alpha}{2}\right) = -BC > 0,$$

since at $v_s = (1 - \alpha)/2$, we have $A = 0$. In addition, the continuity of $G(v_s)$ on $(0, (1 - \alpha)/2)$ guarantees that there is at least one root v^{**} in $(0, (1 - \alpha)/2)$ such that $G(v^{**}) = 0$. Therefore, for $v_s \in (v^{**}, (1 - \alpha)/2)$, we have $AD - BC > 0$.

THEOREM 2.9 *Assume that* $h(v, n) = v(\alpha + 1)/(\alpha + v)$, $\delta(n) = \delta + \nu n$, $f(v) = 1 - v$, *and* $\chi = 0$. (i) *Then at least one coexistence steady state* (v_s, n_s) *exists*; (ii) *there exists a* $\tilde{v} < (1 - \alpha)/2$ *such that for all* $v_s \in (\tilde{v}, (1 - \alpha)/2)$, *we have* $A + D < 0$ *and* $AD - BC > 0$; (iii) *there exists* $\epsilon_1 > 0$ *such that for each* $\epsilon < \epsilon_1$, *there exists a non-empty interval* $[k_1, k_2]$ *of unstable modes*, *so we may expect diffusion-driven instability about the coexistence steady state*; (iv) *if* $\epsilon > \epsilon_1$, *then* (v_s, n_s) *is linearly stable.*

Proof Property (i) was shown in Lemma 2.7. (ii) It was also shown that for $v_s \in (v^*, (1 - \alpha)/2)$, we have $A + D < 0$ and for $v_s \in (v^{**}, (1 - \alpha)/2)$, $AD - BC > 0$. Hence, we define $\tilde{v} = \max(v^*, v^{**})$, so for $v_s \in (\tilde{v}, (1 - \alpha)/2)$, we have $A + D < 0$ and $AD - BC > 0$.

(iii) Now $M_2(k^2)$ is

$$M_2(k^2) = (-\epsilon k^2 + A)(-k^2 + D) - BC,$$

with $A = 1 - 2v_s - n_s(\alpha + 1)\alpha/(\alpha + v_s)^2$, $B = -v_s(\alpha + 1)/(\alpha + v_s) < 0$, $C = \gamma n_s(\alpha + 1)\alpha/(\alpha + v_s)^2 > 0$, and $D = -\gamma n_s \nu < 0$.

If $\epsilon \geq 1$, then $D < 0$ gives $A + D\epsilon \leq A + D < 0$, hence $M_2(k^2)$ is always positive, which results in no diffusion-driven instability for $\epsilon \geq 1$. Therefore, ϵ should be strictly less than 1. Indeed, setting $\epsilon_0 = v_s(1 - \alpha - 2v_s)/\gamma((\alpha + 1 - \delta)v_s - \delta\alpha)$, then for $\epsilon < \epsilon_0$, we have $A + D\epsilon > 0$ and $M_2(k^2)$ can be negative for some k.

By setting $T = k^2$, we have a quadratic form of $M_2(T)$, that is, $M_2(T) = AD - BC + \epsilon T^2 - (A + D\epsilon)T$. Solving this quadratic form gives that there are two positive ϵ, say ϵ_1 and ϵ_2 with $\epsilon_1 < \epsilon_2$, such that for $\epsilon < \epsilon_1$, $M_2(T)$ has two positive roots, say T_1 and T_2 with $T_1 < T_2$. Therefore, $M_2(T)$ is negative for $k \in (k_1, k_2)$ with $k_1 = \sqrt{T_1}$ and $k_2 = \sqrt{T_2}$. For unstable modes $k \in [k_1, k_2]$, we have $\mathrm{Re}(\lambda) > 0$. Hence we may expect diffusion-driven instability about a coexistence steady state (v_s, n_s).

(iv) If $\epsilon > \epsilon_1$, then $M_2(k^2)$ is always positive for all k. Hence, we cannot expect diffusion-driven instability about the coexistence steady state. ■

For $\chi \neq 0$, we obtain a similar result as in Section 2.2.

LEMMA 2.10 *Assume that instability conditions of Theorem* 2.9 *are satisfied. Then we define*

$$\chi^* = \frac{-2v_s^2 + (1 - \alpha + \epsilon\gamma(\delta - \alpha - 1)v_s + \epsilon\gamma\delta\alpha}{(\alpha + 1)v_s n_s}$$

such that a coexistence steady state (v_s, n_s) *for system* (1) *and* (2) *is linearly stable for each* $\chi \geq \chi^*$. *For* $\chi < \chi^*$, *there may exist an interval* $[k_1, k_2]$ *of unstable modes.*

Proof See Lemma 2.1 ■

Figure 10 demonstrates that the stable coexistence steady state without dispersal terms becomes unstable when diffusion terms are introduced (Theorem 2.9). As a result, patterns are generated. It is shown that when we introduce a large prey-taxis term, patterns are disappearing (Lemma 2.10 and see [17] for figure).

2.6. *Type II functional response, constant predator death rate, and logistic growth*

We now modify the analysis of the previous subsection to include a constant rather than density-dependent predator death rate. This does not allow for the possibility of pattern formation (Table 1, row 5). We consider type II functional response, $h(v, n) = (\alpha + 1)/(\alpha + v)v$ as in [27], a constant predator death rate, $\delta(n) = \delta$, and logistic growth for the prey, $f(v) = 1 - v$. Thus the coexistence

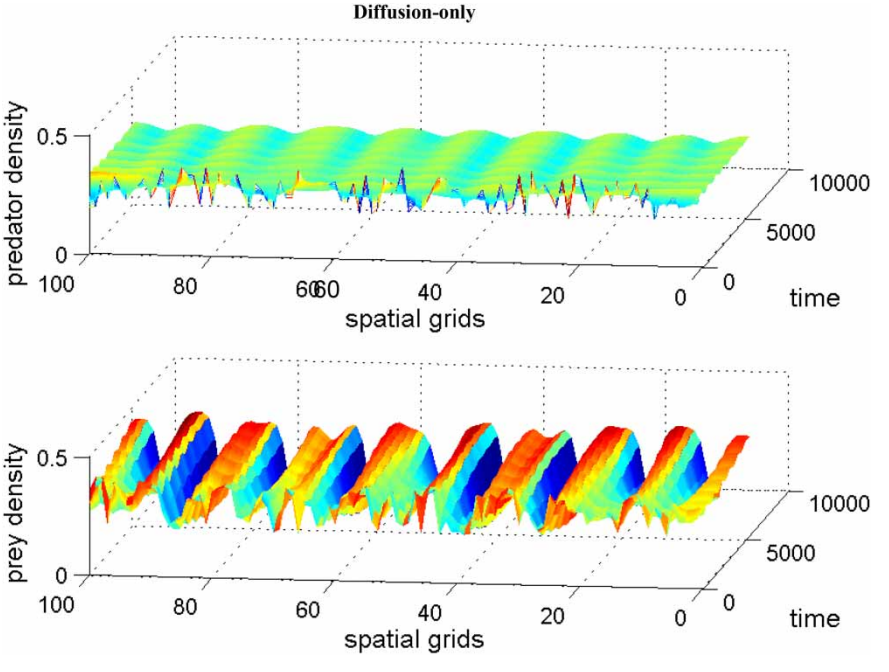

Figure 10. Coexistence steady state is shown to be asymptotically unstable for system (1) and (2) with $\chi = 0$, $f(v) = 1 - v$, $h(v, n) = v(\alpha + 1)/(\alpha + v)$, and $\delta(n) = \delta + \nu n$ with $\alpha = 0.2$, $\delta = 0.6$, $\gamma = 1.2$, and $\nu = 0.4$. The diffusion coefficient ϵ is 0.01. Spatial grid size $dx = 0.25$ and time step $dt = 0.01$ with 60 time units. Here the coexistence steady state is $(v_s, n_s) = (0.296, 0.291)$. Available in colour online.

steady state is

$$(v_s, n_s) = \left(\frac{\delta\alpha}{(1+\alpha-\delta)}, \frac{(1+\alpha)\alpha(1-\delta)}{(1+\alpha-\delta)^2} \right),$$

which is biologically relevant for $0 \leq \delta < 1$. In this case,

$$A = -\frac{\delta(\alpha - 1 + \delta)}{(1+\alpha-\delta)}, \quad B = -\delta, \quad C = \gamma(1-\delta), \quad D = 0,$$

and consequently,

$$M_2(k^2) = \delta\gamma(1-\delta) + \epsilon k^4 + \left(\frac{\delta(\alpha - 1 + \delta)}{(1+\alpha-\delta)} + \delta\chi n_s \right) k^2 > 0$$

for all k. Thus the homogeneous steady state is linearly stable.

It is noted that type II functional response does not play any role in pattern formation versus type I. In a numerical solution (not shown) with $\chi = 6.5$ and a randomly chosen initial distribution, we observe that the solution converges to the coexistence equilibrium $(v_s, n_s) = (0.6, 0.2667)$.

2.7. *Type I functional response, density-dependent predator death rate, and logistic growth*

We now modify the analysis of Section 2.5 to include a type I rather than type II functional response. This also does not allow for the possibility of pattern formation (Table 1, row 6). We include competition in the predator death rate, so the predator death rate is $\delta(n) = \delta + \nu n$. In addition, we consider type I functional response, $h(v, n) = v$, and logistic growth for the prey, $f(v) = 1 - v$. Thus the coexistence steady state is $(v_s, n_s) = ((\delta + \nu)/(1 + \nu), (1 - \delta)/(1 + \nu))$, which is biologically relevant for $0 \leq \delta < 1$. In this case, we obtain

$$A = -\frac{\delta + \nu}{1 + \nu}, \quad B = -\frac{\delta + \nu}{1 + \nu}, \quad C = \gamma\frac{1 - \delta}{1 + \nu}, \quad D = -\nu\gamma\frac{1 - \delta}{1 + \nu}.$$

We find $A < 0$ and $D < 0$ for biologically relevant δ, which result in $A + D < 0$. Moreover, $B < 0$ and $C > 0$ give rise to $AD - BC > 0$. In addition, $A < 0$, $D < 0$, $B < 0$, and $AD - BC > 0$ give $M_2(k^2) = AD - BC + \epsilon k^4 - (A + \epsilon D + B\chi n_s)k^2 > 0$ for all k. Hence, we note that $M_2(k^2) > 0$ for all k, hence the homogeneous steady state is linearly stable.

This result was also confirmed numerically for selected parameter values (not shown here).

3. Global stability

In the previous section, we showed that without both the Allee effect and the density-dependent predator death rate, diffusion, and prey-taxis do not change the local stability of the coexistence steady state. We choose one of the cases without pattern formation to study the global stability of (v_s, n_s). We consider logistic growth for the prey, $f(v) = 1 - v$, a type I functional response, $h(v, n) = v$, a density-dependent predator death rate, $\delta(n) = \delta + \nu n$, and a non-constant prey sensitivity, $\chi(v) = b/v$, for the spatially homogeneous case of system (1) and (2) on an interval $\Omega = [0, L]$ with homogeneous Neumann boundary conditions (3). The following Lyapunov

function,

$$\tilde{V}(v,n) = \int_{v_s}^{v} \frac{\tilde{v}-v_s}{\tilde{v}}\mathrm{d}\tilde{v} + \int_{n_s}^{n} \frac{\tilde{n}-n_s}{\gamma\tilde{n}}\mathrm{d}\tilde{n},$$
$$= v - v_s\ln(v) - v_s + v_s\ln(v_s) + \frac{n - n_s\ln(n) - n_s + n_s\ln(n_s)}{\gamma}, \tag{20}$$

has been used to show the global stability of (v_s, n_s) [5]. We will show that $V(v,n) = \int_\Omega \tilde{V}(v,n)\,\mathrm{d}x$ is a Lyapunov functional for the spatially dependent problem (1) and (2) in this case.

THEOREM 3.1 *Let $f(v) = 1 - v$, $h(v,n) = v$, $\delta(n) = \delta + \nu n$, and $\chi(v) = b/v$, with boundary condition* (3). *We assume that $4\epsilon\gamma > (n_s/v_s)b^2$, then the functional $V(v,n)$ defined in Equation* (20) *is a strong Lyapunov function for system* (1) *and* (2). *The sets $N_L = \{(v,n)|V(v,n) \le L\}$ are positively invariant and (v_s, n_s) is globally asymptotically stable.*

Proof Setting $N_L = \{(v,n)|V(v,n) \le L\}$ for L large enough, then we claim that the sets N_L are positive invariant. When $(v,n) = (v_s, n_s)$, $V(v_s, n_s)$ becomes zero due to $\tilde{V} = 0$. For $v > v_s$, the first term of Equation (20) is positive. Similarly, the second term of (20) is positive. Therefore, $\tilde{V}$ is positive in N_L. Hence, the functional, $V(v,n)$, is bounded below by zero. Moreover, the definition of the Lyapunov functional,

$$\tilde{V} = v - v_s\ln(v) - v_s + v_s\ln(v_s) + \frac{n - n_s\ln(n) - n_s + n_s\ln(n_s)}{\gamma}$$

leads to $\lim_{v\to 0, n\to 0} V(v,n) = \infty$ and $\lim_{v\to\infty, n\to\infty} V(v,n) = \infty$. Since

$$\frac{\partial V(v,n)}{\partial v} = \int_\Omega \frac{v-v_s}{v}\,\mathrm{d}x \quad \text{and} \quad \frac{\partial V(v,n)}{\partial n} = \int_\Omega \frac{n-n_s}{\gamma n}\,\mathrm{d}x,$$

$V(v,n)$ is continuously differentiable for $v, n > 0$. The next step is showing that for $(v,n) \in N_L$, $\mathrm{d}V/\mathrm{d}t$ is negative definite for a certain parameter space.

$$\begin{aligned}\frac{\mathrm{d}V}{\mathrm{d}t} &= \int_\Omega \frac{\mathrm{d}\tilde{V}(v,n)}{\mathrm{d}t}\,\mathrm{d}x \\ &= \int_\Omega \frac{v-v_s}{v}\dot{v} + \frac{n-n_s}{\gamma n}\dot{n}\,\mathrm{d}x \\ &= \int_\Omega \frac{v-v_s}{v}v_{xx} + (v-v_s)(f(v)-n)\,\mathrm{d}x \\ &\quad + \int_\Omega \frac{n-n_s}{\gamma n}(\epsilon n_{xx} - (\chi(v)v_x n)_x) + (n-n_s)(v-\delta-\nu n)\,\mathrm{d}x.\end{aligned} \tag{21}$$

We arrange the right-hand side of this equation into two parts; one including the local dynamics and the other including the dispersal terms. First we look at the local dynamics

$$\begin{aligned}
&\int_\Omega (v - v_s)(f(v) - n) + (n - n_s)(v - \delta - \nu n)\,\mathrm{d}x \\
&\quad = \int_\Omega (v - v_s)(f(v) - n_s + n_s - n) + (n - n_s)(v - \delta - \nu n)\,\mathrm{d}x \\
&\quad = \int_\Omega (v - v_s)(f(v) - n_s) + (n - n_s)(v - \delta - \nu n - v + v_s)\,\mathrm{d}x \\
&\quad = \int_\Omega (v - v_s)(f(v) - f(v_s)) + (n - n_s)(v_s - \delta - \nu n)\,\mathrm{d}x
\end{aligned}$$

(see also [5] for the case of a constant death rate of the predator). Here $(v - v_s)$ and $(f(v) - f(v_s))$ have the opposite sign with $f(v) = 1 - v$ so that $(v - v_s)(f(v) - f(v_s))$ is negative. Similarly, $(n - n_s)$ and $(v_s - \delta - \nu n)$ have the opposite sign due to $(v_s - \delta - \nu n) = \nu(n_s - n)$. Therefore, $\int_\Omega (v - v_s)(f(v) - n) + (n - n_s)(v - \delta - \nu n)\,\mathrm{d}x$ is negative unless $(v, n) = (v_s, n_s)$. We now take into account the dispersal term of (21) by using integration by parts with zero flux boundary condition

$$\begin{aligned}
&\int_\Omega \frac{v - v_s}{v} v_{xx} + \frac{n - n_s}{\gamma n}(\epsilon n_{xx} - (\chi(v) v_x n)_x)\,\mathrm{d}x \\
&\quad = -\int_\Omega \left(\frac{v - v_s}{v}\right)_v (v_x)^2 + \epsilon \left(\frac{n - n_s}{\gamma n}\right)_n (n_x)^2 - \left(\frac{n - n_s}{\gamma n}\right)_n \chi(v) n v_x n_x\,\mathrm{d}x \\
&\quad = -\int_\Omega \frac{v_s}{v^2}(v_x)^2 + \epsilon \frac{n_s}{\gamma n^2}(n_x)^2 - \frac{n_s}{\gamma n}\chi(v) v_x n_x\,\mathrm{d}x \\
&\quad = -\int_\Omega X^T A X\,\mathrm{d}x,
\end{aligned}$$

where

$$X = \begin{pmatrix} v_x \\ n_x \end{pmatrix} \quad \text{and} \quad A = \begin{pmatrix} \dfrac{v_s}{v^2} & -\dfrac{n_s}{2\gamma n}\chi(v) \\ -\dfrac{n_s}{2\gamma n}\chi(v) & \epsilon \dfrac{n_s}{\gamma n^2} \end{pmatrix}.$$

Thus, the matrix A is symmetric. Hence, if A is positive definite, all eigenvalues of the matrix A are positive. Here $\mathrm{tr}(A) = v_s/v^2 + \epsilon(n_s/\gamma n^2)$ is positive. Thus a positive determinant

$$\Delta(A) = \frac{v_s}{v^2}\epsilon\frac{n_s}{\gamma n^2} - \frac{n_s^2}{4\gamma^2 n^2}\chi(v)^2$$

guarantees two positive eigenvalues for the matrix A. As a result, for $(v, n) \in N_L$ $(\mathrm{d}V/\mathrm{d}t) < 0$. With the specific example of $\chi(v) = b/v$, we have the condition for positive eigenvalues that $4\epsilon\gamma > (n_s/v_s)b^2$. For the special case of $\chi(v) = 0$, i.e. diffusion-only case, the matrix A is always positive definite for N_L. Therefore, the functional $V(v, n)$ is shown to be a Lyapunov functional under the condition specified above. Thus, $V(v, n) \to 0$ as $t \to \infty$, so $v \to v_s$ and $n \to n_s$. Therefore, the homogeneous steady state (v_s, n_s) is globally asymptotically stable. ■

4. Conclusion

In this paper, we considered pattern formation for a predator–prey taxis model of reaction–diffusion–advection type given by (1) and (2). We considered various reaction terms: for the predator term they include type I and type II functional responses as well as ratio-dependent functional responses. We considered constant and density-dependent death rate of the predator and logistic growth or an Allee-type growth for the prey.

In summary, the following functional forms support spatial pattern formation:

(i) a density-dependent death rate, e.g. $\delta(n) = \delta + \nu n$, and an Allee effect, e.g. $f(v) = K(1 - v)(v - a)$, and a type I functional response, e.g. $h(v, n) = v$:
- patterns form with no prey-taxis (Section 2.1),
- patterns persist with small prey-taxis but disappears for large prey-taxis (Section 2.2),
- patterns disappear when Allee dynamics are replaced by logistic dynamics (Section 2.7),

(ii) a hyperbolic ratio-dependent functional response, e.g. $h(v, n) = \mu v/(dn + v)$ and logistic growth, e.g. $f(v) = 1 - v$:
- patterns form with no prey-taxis (Section 2.4),
- patterns persist with small prey-taxis but disappears for large prey-taxis (Section 2.4),
- patterns disappear if a hyperbolic functional response is replaced by a linear functional response (Section 2.3);

(iii) a density-dependent death rate, e.g. $\delta(n) = \delta + \nu n$, and a type II functional response, e.g. $h(v, n) = (\alpha + 1)v/(v + \alpha)$.
- patterns form with no prey-taxis (Section 2.5),
- patterns persist with small prey-taxis but disappears for large prey-taxis (Section 2.5),
- patterns disappear if a density-dependent predator death rate is replaced by a constant predator death rate (Section 2.6).

The significance of this research is as follows; contrary to a diffusion process that may give rise to pattern formation, prey-taxis tends to stabilize predator–prey interactions (Theorem 2.3). In the long run, prey-taxis tends to transform heterogeneous environments into homogeneous environments, which gives an opposite result to the chemotaxis case. Under strong chemotactic sensitivity, amoebae tend to aggregate [29]. Hence the role of taxis may be strongly related to the local population dynamics of the species.

In this paper, prey-taxis is shown to tend to reduce the likelihood of pattern formation in spatial predator–prey systems, but other kinds of taxis may have the opposite effect on pattern formation. For example, we may investigate prey defences. Prey tend to adjust their relative position to the predator to reduce predation risk [10,24,37,38]. We may apply the concept of prey-taxis to prey escape response to predator density. It may refer to predator-taxis. For instance, crayfish (prey) exhibit different activities depending on the presence of a predator (bass). An increased predation risk restricts crayfish foraging and increases anti-predator behaviour such as shelter seeking [8,11]. Another interesting taxis is that predators may attract their prey to come nearby [31]. In this case, prey move towards predators. As a conjecture, from Equation (8), we may predict that positive predator-taxis (away from predators) tends to generate pattern formation but negative predator-taxis (towards predators) tends to inhibit pattern formation. However, the detailed argument is left for future work.

Acknowledgements

We thank G. de Vries, C. Cosner, and C.J. Bampfylde for helpful discussion and comments on the manuscript. We appreciate two anonymous reviewers for helpful comments and suggestions. We would also like to thank all the members of the Lewis lab for encouragement and feedback, which have improved this research. JML was supported by a University

of Alberta Studentship and by an NSERC collaborative Research Opportunity Grant. TH was supported by NSERC. ML was supported by NSERC and a Canada Research Chair.

References

[1] M.B. Allen and M.B. Eli, *Numerical Analysis for Applied Science*, Wiley-Interscience, New York, 1998.
[2] D. Alonso, F. Bartemeus, and J. Catalan, *Mutual interference between predators can give rise to Turing spatial patterns*, Ecology, 83 (2002), pp. 28–34.
[3] R. Arditi, Y. Tyutyunov, A. Morgulis, and V. Govorukhin, *Directed movement of predators and the emergence of density-dependence in predator-prey models*, Theoret. Population Biol. 59 (2001), pp. 207–221.
[4] V.N. Biktashev, J. Brindley, A.V. Holden, and M.A. Tsyganov, *Pursuit-evasion predator-prey waves in two spatial dimensions*, Chaos 91 (2004), p. 218102.
[5] N.F. Britton, *Reaction-Diffusion Equations and Their Applications to Biology*. Academic Press, London, 1986.
[6] A. Chakraborty, M. Singh, D. Lucy, and P. Ridland, *Predator-prey model with prey-taxis and diffusion*, Math. Comput. Model. 46 (2007), pp. 482–498.
[7] Y. Dolak and T. Hillen, *Cattaneo models for chemosensitive movement numerical solution and pattern formation*, J. Math. Biol. 46 (2003), pp. 153–170.
[8] J.E. Garvey, R.A. Stein, and H.M. Thomas, *Assessing how fish predation and interspecific prey competition influence a crayfish assemblage*, Ecology 75(2) (1994), pp. 532–547.
[9] D. Grunbaum, *Using spatially explicit models to characterize foraging performance in heterogeneous landscapes*, Am. Nat. 151 (1998), pp. 97–115.
[10] W.D. Hamilton, *Geometry for the selfish herd*, J. Theor. Biol. 31 (1971), pp. 295–311.
[11] A.M. Hill and D.M. Lodge, *Replacement of resident crayfishes by an exotic crayfish: the roles of competition and predation*, Ecol. Appl. 9(2) (1999), pp. 678–690.
[12] T. Hillen and K. Painter, *Global existence for a parabolic chemotaxis model with prevention of overcrowding*, Adv. Appl. Math. 26(4) (2001), pp. 280–301.
[13] J. Jorné, *The effects of ionic migration on oscillations and pattern formation in chemical systems*, J. Theor. Biol. 43 (1974), pp. 375–380.
[14] P. Kareiva and G. Odell, *Swarms of predators exhibit 'preytaxis' if individual predators use arearestricted search*, Am. Nat. 130 (1987), 233–270.
[15] T. Kolokolnikov, T. Erneux, and J. Wei, *Mesa-type patterns in the one-dimensional brusselator and their stability*, Phys. D 214 (2006), pp. 63–77.
[16] A. Kurganov and E. Tadmor, *New high resolution central schemes for nonlinear conservation laws and convection-diffusion equations*, J. Comput. Phys. 160 (2000), pp. 214–282.
[17] J. Lee, *Prey-taxis and its applications*, Ph.D. thesis, University of Alberta, Edmonton, AB, Canada, 2006.
[18] J. Lee, T. Hillen, and M.A. Lewis, *Prey-taxis equations: continuous travelling waves for pest control*, in preparation, 2007.
[19] R.J. LeVeque, *Finite Volume Methods for Hyperbolic Problems*, Cambridge University Press, Cambridge, 2002.
[20] M.A. Lewis, *Spatial coupling of plant and herbivore dynamics: the contribution of herbivore dispersal to transient and persistent 'waves' of damage*, Theor. Population Biol. 45 (1994), pp. 277–312.
[21] J.E. Losey and R.F. Denno, *The escape response of pen aphids to foliar-foraging predators: factors affecting dropping behaviour*, Eco. Entom. 23 (1998c), pp. 53–61.
[22] H. Malchow, *Flow-and locomotion-induced pattern formation in nonlinear population dynamics*, Ecol. Model. 82 (1995), pp. 257–264.
[23] H. Malchow, *Motional instability in prey-predator system*, J. Theor. Biol. 204 (2000), pp. 639–647.
[24] T.L. Morton, J. Haefner, V. Nugala, R.D. Decino, and L. Mendes, *The selfish herd revisited: do simple movement rules reduce relative predation risk*, J. Theor. Biol. 167 (1994) pp. 73–79.
[25] J.D. Murray, *Mathematical Biology*, Springer Verlag, New York, 1989.
[26] A. Okubo and S.A. Levin, *Diffusion and Ecological Problems: New Perspectives*, 2nd ed., Springer Verlag, New York, 2000.
[27] M.R. Owen and M.A. Lewis, *How predation can slow, stop or reverse a prey invasion*, Bull. Math. Biol. 63 (2001), pp. 655–684.
[28] A.B. Rovinsky and M. Menzinger, *Chemical instability induced by a differential flow*, Phys. Rev. Lett. 69 (1992), pp. 1193–1196.
[29] L.A. Segel, ed., *Mathematical Models in Molecular and Cellular Biology*, Cambridge University Press, Cambridge, 1980.
[30] L.A. Segel and J. Jackson, *Dissipative structure: an explanation and an ecological example*, J. Theor. Biol. 37 (1972), pp. 545–559.
[31] W. Shi and D.R. Zusman, *Fatal attraction*, Nat. Sci. Correspondence 366 (1993), pp. 414–415.
[32] J.C. Strikwerda, *Finite Difference Schemes and Partial Differential Equations*, Wadsworth, Inc., CA, 1989.
[33] M.A. Tsyganov, J. Brindley, A.V. Holden, and V.N. Biktashev, *Quasisoliton interaction of pursuitevasion waves in a predator-prey system*, Phys. Rev. Lett. 91 (2003), pp. 218102.
[34] P. Turchin, *Complex Population Dynamics*, Princeton University Press, Princeton and Oxford, 2003.

[35] R. Tyson, S.R. Lubkin, and J.D. Murray, *Model and analysis of chemotactic bacterial patterns in a liquid medium*, J. Math. Biol. 38 (1999), pp. 359–375.
[36] R. Tyson, L.G. Stern, and R.J. LeVeque, *Fractional step methods applied to a chemotaxis model*, J. Math. Biol. 41 (2000), pp. 455–475.
[37] S.V. Viscido and D.S. Wethey, *Quantitative analysis of fiddler crab flock movement: evidence for 'selfish herd' behaviour*. Anim. Behav. 63 (2002) pp. 735–741.
[38] S.V. Viscido, M. Miller, and D.S. Wethey, *The response of a selfish herd to an attack from outside the group perimeter*, J. Theor. Biol. 208 (2001), pp. 315–328.